JOURNAL OF PHYSICAL ORGANIC CHEMISTRY
J. Phys. Org. Chem. 2007; **20:** 285–295
Published online 30 March 2007 in Wiley InterScience
(www.interscience.wiley.com) DOI: 10.1002/poc.1165

Bis-4,9-diazapyrenium dications: synthesis of the methylenedibenzyl-analogue, interactions with nucleotides, DNA, RNA. The antitumour activity of all till now prepared analogues

Ivo Piantanida,[1]* Mladen Žinić,[1] Saška Marczi[2] and Ljubica Glavaš-Obrovac[3,4]

[1]Laboratory for Supramolecular and Nucleoside Chemistry, Ruđer Bošković Institute, HR-10002 Zagreb, Croatia
[2]Scientific Unit for Medical Research, Clinical Hospital Osijek, J. Huttlera 4, 31000 Osijek, Croatia
[3]Department of Nuclear Medicine and Pathophysiology, Clinical Hospital Osijek, J. Huttlera 4, 31000 Osijek, Croatia
[4]Department of Medicinal Chemistry and Biochemistry, School of Medicine Osijek, J. Huttlera 4, 31000 Osijek, Croatia

Received 20 September 2006; revised 15 December 2006; accepted 15 January 2007

ABSTRACT: Novel bis-4,9-diazapyrenium dication has shown reversible pH dependent formation of 4,9-diazapyrenium pseudobase in water characteristic for most 4,9-diazapyrenium derivatives. The compound has formed non-covalent complexes with nucleotides in water, whose stability is controlled dominantly by aromatic stacking interactions. No cooperativity between two 4,9-diazapyrenium subunits was observed in binding of nucleotides. Novel bis-4,9-diazapyrenium dication formed mono-intercalative complexes with studied double stranded DNA and RNA. Additional interactions of non-intercalated part were found to depend significantly on the polynucleotide secondary structure, yielding strong DNA over RNA preference. Appearance of ICD band of **3** was found to be specific for DNA polynucleotides and together with observed destabilisation of double stranded RNA is attributed to the aggregation of compound in one of the RNA grooves. All bis-4,9-diazapyrenium dications prepared till now have shown considerable antiproliferative activity against five human tumour cell lines, which suggested mechanism of action by interacting with cell DNA. Copyright © 2007 John Wiley & Sons, Ltd.

KEYWORDS: bis-4,9-diazapyrenium cations; DNA; RNA; intercalation; antiproliferative activity; antitumour activity

INTRODUCTION

In the last 40 years, small molecules that intercalate into DNA and RNA have been the target of the most intensive research. They have been studied for their usage as the fluorescent markers for nucleic acids, molecular tools (artificial endonucleases, etc.), or simply due to broad spectra of their biological activities.[1,2] The recently discovered relatively selective interaction of ethidium bromide (EB) and it's close analogues with particular RNA, HIV-related sequences[3] stirs new interest for re-investigation of already known aromatic systems[4] and their close analogues,[5] since it was shown that even small structural variation can strongly influence the activity of compounds. In the last decade, 2,7-diazapyrenium derivatives (2,7-DAPs), actually structural analogues of pyrene and methyl-viologen, have shown interesting specificity and cleaving properties of the double stranded polynucleotides, offering possible implementation as artificial endonucleases.[6] In addition, 4,9-diazapyrenium cations (4,9-DAPs) can be considered as derivatives of EB with extended aromatic surface. At variance to 2,7-DAPs and EB derivatives, 4,9-DAPs reveal dramatically different physico-chemical properties, among which the pH dependent opening of the heteroaromatic ring is the most prominent[7] and should be stressed as the possible cause of the observed selectivity towards tumour cell lines.[8] Monomeric 4,9-DAPs intercalate into double stranded and single stranded DNA and RNA, their affinity and specificity being strongly dependent on the attached substituents.[9,10] Substituents on the 4,9-DAP moiety also have strong impact on their antitumour activity.[8] A DNA/RNA bis-intercalating compounds are one of the most extensively studied groups of small molecules,[11] offering a number of advantages if compared to mono-intercalators. There is intriguing difference in nucleotide binding between dimeric 2,7-DAPs and their 4,9-DAP analogues. Former bind nucleotide by pronounced chelate effect (nucleobase placed between DAP units, simultaneous aromatic stacking interactions)[6f], while for the

**Correspondence to:* I. Piantanida, Laboratory for Supramolecular and Nucleoside Chemistry, Ruđer Bošković Institute, P.O.B. 180, HR-10002 Zagreb, Croatia.
E-mail: pianta@irb.hr

latter (bis-4,9-DAP) molecules the chelate effect is not observed.[9] As an extension of studies of a linker contribution on the mode of binding dimeric 4,9-DAPs to the nucleotides and polynucleotides, here we present synthesis of the derivative with the 2,2′-(methylenedibenzyl)-linker and study of interactions with nucleotides and DNA/RNA. Also, here are presented the effects of all till now known bis-4,9-diazapyrenium dications on the growth of five human tumour cell lines.

CHEMISTRY

Synthesis

Starting material 4,9-diazapyrene **1** has been prepared using the modified Mosby procedure[7,12] based on double cyclisation of the respective biphenyl 2,2′-diamides in $AlCl_3$/NaCl melt at 250–270°C. The 2,2′-(methylenedibenzyl)-bis-(4,9-diazapyrenium) dibromide **3** was prepared by reacting 2.2 equivalents of **1** with bis4-(bromomethyl)phenyl]methane **2** (Scheme 1) under similar conditions as used for previously prepared m- and p-xylylene bis-4,9-diazapyrenium analogues (**5**, **6**; Scheme 2).[7] For comparison of spectroscopic properties with previously studied **5** and **6**, dibromide **3** was converted into corresponding dichloride **4** by anion exchange with freshly prepared AgCl. Hygroscopic nature of **3** and **4** hampered elemental analysis; however, the structures were confirmed by one- and two-dimensional NMR techniques analogously with previously reported bis-4,9-diazapyrenium analogues[7] and ESI-MS data. Aqueous solutions of **3**, **4** were found to be stable on a cool and dark place for up to 3 days, after that time slow degradation of 4,9-diazapyrenium ring started to show up in ^{1}H-NMR spectra.

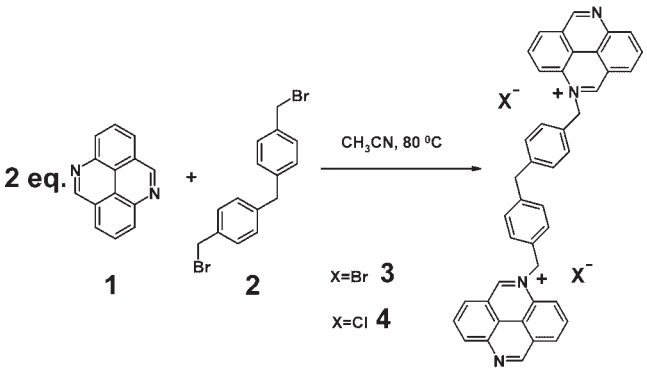

Scheme 1. Synthesis of **3** and **4**

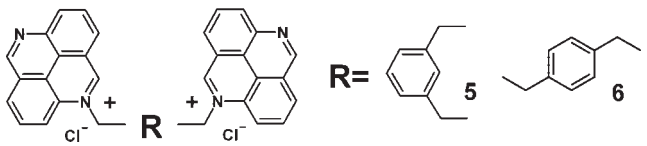

Scheme 2. Previously studied bis-4,9-diazapyrenium derivatives **5** and **6**[7,9]

Spectroscopy

The UV/Vis spectra of **3** and **4** were found to be identical and taken in bi-distilled water ($c = 2{\cdot}10^{-5}$ mol dm^{-3}) are characterised by following maxima λ_{max}/nm (ε/mol^{-1} cm^2): 235.5 (101.2), 281 (18.95), 355 (15.7), 392 (15.9). Molar extinction coefficients (ε) of **3** and **4** are approximately double than found for corresponding 4,9-diazapyrenium 'monomer',[7] pointing that there is no intramolecular stacking between diazapyrenium subunits of **3** and **4**. Also, the UV/Vis spectra of **3** and **4** are identical to those of previously studied analogues **5** and **6**.[7] Absorption of all maxima is linearly dependent on a concentration up to $c(\mathbf{3},\mathbf{4}) = 5{\cdot}10^{-5}$ mol dm^{-3}, pointing that there is no intermolecular stacking. Nevertheless, at $c(\mathbf{3},\mathbf{4}) = 5{\cdot}10^{-5} - 1{\cdot}10^{-4}$ mol dm^{-3} small hypochromic effect is observed (5%), suggesting that intermolecular interactions between molecules of **3** or **4** start to take place. Insufficient solubility of **3** and **4** didn't allow collection of enough data points for accurate calculation of self-association constant K_a. Similar as all previously studied 4,9-diazapyrenium derivatives,[7] **3** and **4** show strong fluorescence in aqueous solution. Again, fluorescence maximum ($\lambda_{em} = 430$ nm) and emission intensity of **3** and **4** resemble closely to the previously studied analogues **5** and **6**. Excitation spectra of **3** and **4** were found to be in good agreement with the corresponding electronic absorption spectra, proving that chromophores responsible for absorption of the light are also emitting fluorescence.

Reversible pH dependent formation of 4,9-diazapyrenium pseudobase in water

The electronic absorption, ^{1}H-NMR and fluorescence spectra of most mono- and di-cationic 4,9-diazapyrenium salts taken in water showed strong pH dependence. This was explained by reversible formation of corresponding diazapyrenenium mono-pseudobase. The equilibrium constants (expressed as pK_{DMOH}) were calculated from pH dependent changes in electronic absorption spectra. However, *pK* values have shown to be strongly dependent on a type of substituent and it's position on the diazapyrenium ring.[7,10] Therefore, it was necessary to determine the *pK* values of **3** and **4**. This was done by monitoring the changes in UV/Vis spectrum of **3** and **4** while changing the pH in the range of pH 3–8 (Fig. 1). The $pK(\mathbf{3},\mathbf{4}) = 6.4$ calculated from the spectral changes was in good agreement with the *pK* values previously determined for mono-cationic 4,9-diazapyrenium analogues.[7]

DOI: 10.1002/poc

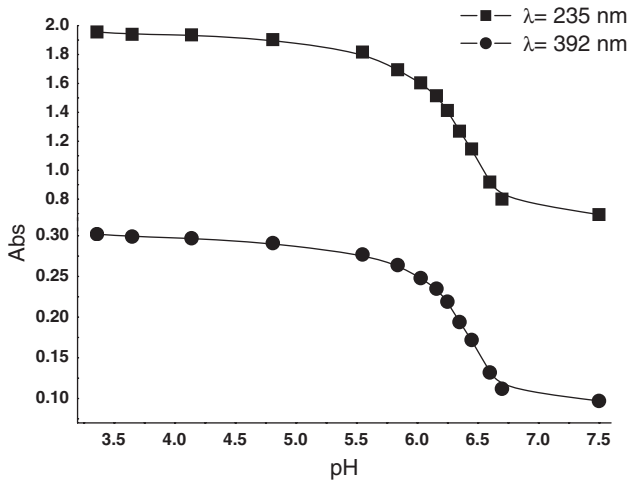

Figure 1. Changes of the electronic absorption spectra of **3** ($c = 2 \times 10^{-5}$ mol dm^{-3}) in water induced by variation of pH = 3–8

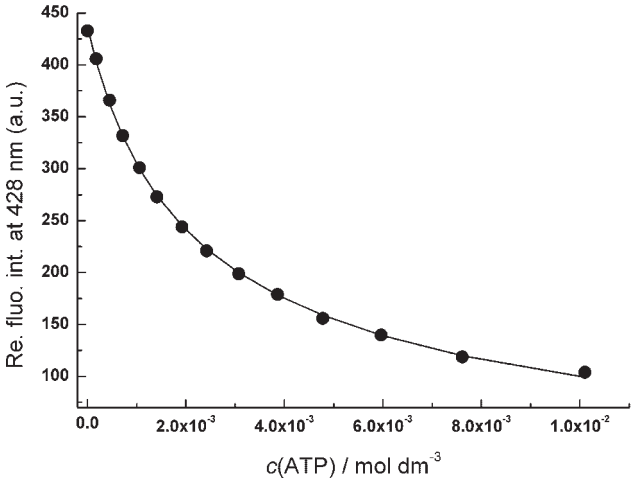

Figure 2. Fluorimetric titration of **3** at $\lambda_{max} = 428$ nm ($c = 4.0 \times 10^{-6}$ mol dm^{-3}) with ATP at pH = 5 (sodium citrate buffer, $I = 0.03$ mol dm^{-3})

Binding of nucleotides in water

Interactions of **4** with nucleotides have been studied by fluorescence titrations in buffered aqueous solution at pH = 5. At these conditions, studied compound is more than 95% in diazapyrenium form ($pK = 6.4$). Consecutive additions of studied nucleotides induced total quenching of fluorescence emission of **4**, similar as noted for previously studied analogues.[7] The binding constants (K_s, Table 1) were calculated from fluorimetric titration data by processing the changes in complete spectra using the SPECFIT program.[13] For all studied nucleotides, the best fit was obtained for the formation of two complexes, namely **4**/nucleotide complex of 1:1 stoichiometry exhibiting weaker fluorescence compared to free **4** and the **4**/(nucleotide)$_2$ being non-fluorescent (Figure 2).

Previous studies have shown that titration with nucleotides resulted in total quenching of all 'monomer' analogues of **4**, as a result of aromatic stacking interactions between nucleobase and 4,9-diazapyrenium moiety. It is interesting to note that previously studied bis-4,9-diazapyrenium (**5**, **6**) analogues,[7] do not form chelate type of complexes with nucleotides, although xylyl-linker should support insertion of one nucleobase between 4,9-DAP units stabilised by simultaneous aromatic stacking interactions.

However, the rigidity and length of the 2,2′-(methylenedibenzyl)-linker of **4** is not likely to allow formation of chelate type of complex where nucleotide forms non-covalent interactions with both diazapyrenium subunits simultaneously. This is in accord with titration results (Table 1), pointing towards formation of two different **4**/nucleotide complexes. At higher [**4**]/[nucleotide] ratios complex of 1:1 stoichiometry is dominant species, only one 4,9-diazapyrenium unit of **4** forming non-covalent interaction with nucleotide. In a such **4**/nucleotide complex, only fluorescence of the 4,9-diazapyrenium unit interacting with nucleobase is totally quenched, while the other diazapyrenium unit is free and emitting fluorescence; as a result 1:1 stoichi-

Table 1. Comparison of binding constants (log K_s)[a] and their fluorimetric properties observed for complexes of **4** and analogues **5**[b] and **6**[b] with different nucleotides[c]

	4				**5**[b]		**6**[b]	
	[d]log K_{s11}	[e]I_{11}/I_0	[d]log K_{s12}	[e]I_{12}	[d]log K_{s11}	[e]I_{11}/I_0	[d]log K_{s11}	[e]I_{11}/I_0
CMP	≈1	0.9	[f]	[f]	1.4	0.5	1.6	0.6
GMP	2.7	0.7	2.3	0	2.1	<0.1	2.3	0.4
AMP	2.6	0.2	2.2	0	2.3	0.5	2.6	<0.1
ATP	2.9	0.4	2.1	0	2.2	0.7	2.9	<0.1

[a] Obtained by SPECFIT Program, error of calculated K_s values is at most ±10%.
[b] Published results.[7]
[c] AMP^{2-} = adenosine monophosphate; ATP^{4-} = adenosine triphosphate; GMP^{2-} = guanosine monophosphate; CMP^{2-} = cytidine monophosphate.
[d] K_{11} and K_{12} refer to the equilibria L + N ⇄ LN and LN + N ⇄ LN_2 (L = ligand; N = nucleotide), respectively.
[e] I_0 is emission intensity of free **4**, I_{11}, and I_{12} are emission intensities calculated by SPECFIT Program for complexes of 1:1 and 1:2 stoichiometry, respectively.
[f] Not determined due to low percentage to complex formed.

DOI: 10.1002/poc

ometry **4**/nucleotide complexes emit fluorescence weaker than free **4** (Table 1). At higher excess of [nucleotide] over [**4**], 1:2 complex [**4**/(nucleotide)$_2$] is progressively formed, in which both 4,9-diazapyrenium units are interacting with two separate molecules of nucleotide and consequently, fluorescence of **4** is totally quenched.

Calculated K_{s11} and K_{s12} values for **4**/nucleotide complexes (Table 1) are of the same order of magnitude and also similar to the previously determined K_s values for mono- and bis-4,9-diazapyrenium (**5**, **6**) analogues.[7] That is in good agreement with the presumption that aromatic subunits of **4** bind nucleotides independently. Stability constant values (K_s) of **4**/nucleotide complexes are dependent on the size of the aromatic surface of nucleobase pointing towards π–π aromatic stacking interactions between **4** and nucleotides as dominant binding interactions.

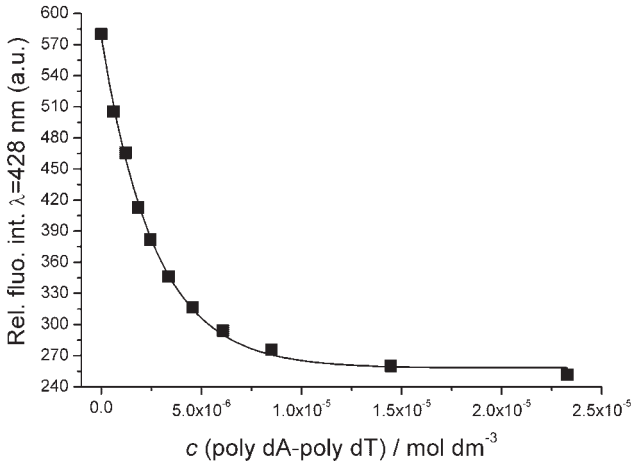

Figure 3. Fluorimetric titration of **3** at $\lambda_{max} = 428$ nm ($c = 8.7 \times 10^{-7}$ mol dm^{-3}) with poly dA-poly dT at pH = 5 (sodium citrate buffer, $I = 0.03$ mol dm^{-3})

Interactions with polynucleotides

Spectrophotometric titrations. UV/Vis titration of **3** and **4** with ct-DNA revealed bathochromic shift of λ_{max} at 392 nm for 30 nm and hypochromic effect of about 30 % in spectra of **3** and **4**. Observed effects strongly suggest involvement of aromatic π–π interactions in binding, most likely due to the intercalation of **3** and **4** as the dominant binding mode.[14] However, systematic deviation from the isosbestic point observed in UV/Vis titration spectra suggested formation of more than one type of **3**,**4**/ct-DNA complex under conditions close to the saturation of intercalation binding sites, possibly due to the simultaneous formation of intercalative and non-intercalative type of complexes.[10,15] Due to the simultaneous formation of at least two complexes it was not possible to process UV/Vis titration data by means of Scatchard equation[16,17] to calculate binding constants (K_s) and ratios $n_{(\text{bound compound}]/[\text{polynucleotide})}$.

To overcome the experimental conditions present in UV/Vis experiments under which more than one **3**,**4**/polynucleotide complex is formed, we have exploited strong fluorescence emission of studied compounds, allowing usage of an order of magnitude of lower concentrations. In this way, it was possible to perform titrations at large excess of the polynucleotide, at which conditions we presumed that one binding mode is dominant. This presumption was confirmed by excellent fitting of the titration data to the Scatchard equation model.[16,17]

Further experiments were done in more detail with **3** due to the somewhat better solubility and few experiments were repeated with **4**, giving essentially the same results as found for **3**. Addition of double stranded DNA polynucleotides induced total quenching of fluorescence emission of **3** at high excess of polynucleotide over **3** (Fig. 3). Processing of titration data by means of Scatchard equation[16,17] gave excellent agreement of experimental and calculated data, pointing towards formation of only one type of **3**/polynucleotide complex.

The obtained K_s values (Table 2) do not differ significantly from the previously reported for mono- and bis-diazapyrenium analogues.[9] Calculated ratios n are of the same order of magnitude as expected for mono-intercalator and significantly higher than theoretically possible values for bis-intercalation ($n_{teor.} < 0.1$).[18] Titration experiments with double stranded RNA poly A-poly U yielded total quenching of fluorescence emission of **3** already at excess of **3** over intercalation binding sites, what hampered processing of the titration data by means of Scatchard equation. Much lower concentrations of poly A-poly U necessary for reaching the end of titration if compared to DNA polynucleotides point either to much higher affinity of **3** towards ds-RNA or simultaneous formation of more different complexes.

Table 2. Binding constants [a](K_s) and ratios [a]$n_{([\text{bound compound}]/[\text{polynucleotide}])}$ calculated from fluorimetric titrations[b] of **3**, **5** and **6**

	3		**5**[d]		**6**[d]	
	n	log K_s	n	log K_s	n	log K_s
ct-DNA	0.3	6.0	0.14	5.8	0.08	7.0
Poly dAdT-poly dAdT	0.2	6.3	—	—	0.16	6.6
Poly dGdC-poly dGdC	0.2	6.4	—	—	0.23	6.6
Poly dA-poly dT	0.3	6.6	—	—	—	—
Poly A-poly U	[c]	[c]	—	—	—	—

[a] Accuracy: $n \pm 10$–30%, K_s vary within the order of magnitude.
[b] pH = 5, sodium citrate buffer, $I = 0.03$ mol dm^{-3}, data processed by means of Scatchard equation.
[c] Not possible to calculate.
[d] Published results.[7]

DOI: 10.1002/poc

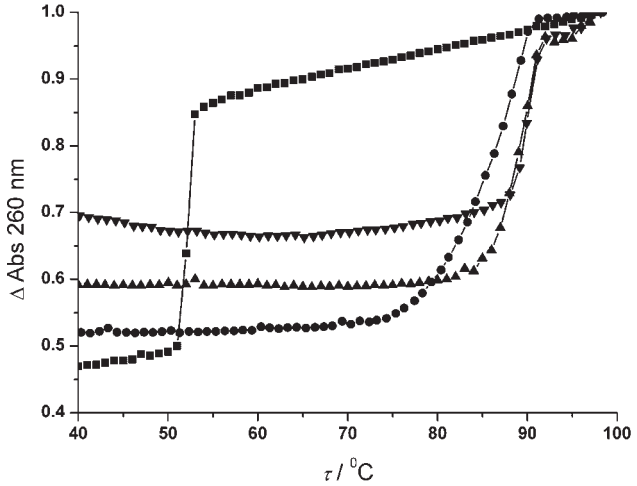

Figure 4. Melting curves of poly dA-poly dT and **3** at pH = 5 (sodium citrate buffer, $I = 0.03\ \text{mol dm}^{-3}$). For measuring conditions see footnotes to Table 3 and the Experimental section; the ratios r ([**3**]/[ct-DNA]) are: 0.0, 0.05, 0.1, 0.2, 0.3, 0.5 (from left to right), and the curves are normalised

Thermal denaturation experiments. Addition of **3** to the DNA ds-polynucleotides yielded exceptionally strong thermal stabilisation of double stranded helices (Fig. 4, Table 3).

On the other hand, addition of **3** to poly A-poly U induced conversion of biphasic thermal denaturation curve into triphasic. The first transition at $T_m = 36.3°C$ (attributed to denaturation of poly A-poly U)[19] was upon addition of **3** converted into two-step transition, first having negative and other positive sign of ΔT_m value compared to T_m value of poly A-poly U. Observed results could only be explained by co-existence of two different binding modes of **3**, one destabilising and another stabilising double helical structure of RNA. It is important to stress that stabilising effect (positive ΔT_m value) was constant over studied range of ratios r, while destabilising effect (negative ΔT_m values) substantially increased with increasing value of r. Stabilisation could be explained by intercalative mode of binding of **3** to ds-RNA, low ΔT_m values (+3.9°C) suggesting that only one 4,9-diazapyrenium unit intercalated into double helix. It is well known that many classical intercalators bind to the ds-polynucleotides also by non-intercalative binding mode at $r_{[\text{compound}]/[\text{polynucleotide}]} > 0.2$.[10,15] Increasing impact of such non-intercalative binding mode is usually proportional to the increase of ratio r, what corresponds here is the observed substantial increase of the negative ΔT_m values. The third transition curve observed in thermal denaturation experiment with poly A-poly U at $T_m = 77.2°C$ (attributed to poly AH^+-poly AH^+)[19] was substantially destabilised by increasing values of ratio r. The reason for that is likely stabilisation of poly A-poly U and in addition high thermal denaturation point of poly AH^+-poly AH^+, at which temperatures **3** very likely does not form a stable complex with poly AH^+-poly AH^+. Also, repulsive forces between positively charged adenines of poly AH^+-poly AH^+ at pH = 5 and two positive charges of **3** could be the cause of destabilisation effect.

To shed more light on the influence of electrostatic interactions on the thermal stabilisation of double helices in the presence of **3**, we have performed thermal melting experiments at increased ionic strength with $c(\text{NaCl}) = 0.1\ \text{mol dm}^{-3}$ in the respective buffer. Obtained results for ds-DNA polynucleotides (Table 3) showed, as expected, increased T_m value for the free DNA and again high stabilisation effect upon addition of **3**. This result points towards dominant role of aromatic stacking interactions between **3** and DNA bases in complex stability, while interactions of positive charges of **3** with negatively charged DNA phosphates play minor (if any) role. The increase of ionic strength completely abolished any effect of **3** on thermal denaturation of poly A-poly U, which suggested that intercalative binding mode (if present at all) plays minor role in the binding of **3** to poly A-poly U.

Table 3. ΔT_m values (°C)[a] of studied ds-polynucleotides at different ratios [b]r of **3** at pH = 5.0 (sodium citrate buffer, $I = 0.03\ \text{mol dm}^{-3}$)

r	0.05	0.1	0.2	0.3
ct-DNA	11.1/23.0	>35[c]	>35[c]	>35[c]
ct-DNA, +0.1 M NaCl	16.6	>22[c]	>22[c]	>22[c]
Poly dA-poly dT	31.4	36.0	37.6	38.0
Poly dA-poly dT+0.1 M NaCl	0	2.4	5.2	8.5
[d]Poly A-poly U	−4.0/+3.9	−5.4/+4.0	−5.9/+3.8	−/+3.9
[d]Poly AH^+-poly AH^+	−1.4	−1.8	−2.7	−4.3
[d]Poly A-poly U	0	0	0	0
[d]Poly AH^+-poly AH^+ + 0.1 M NaCl	0	0	0	0

[a] Error in ΔT_m: ± 0.5°C.
[b] r = [compound]/[polynucleotide].
[c] $T_m > 100°C$.
[d] Biphasic transitions: the first transition at $T_m = 36.3°C$ is attributed to denaturation of poly A-poly U and the second transition at $T_m = 77.2°C$ is attributed to denaturation of poly AH^+-poly AH^+ since poly A at pH = 5 is mostly protonated and forms ds-polynucleotide.[19]

DOI: 10.1002/poc

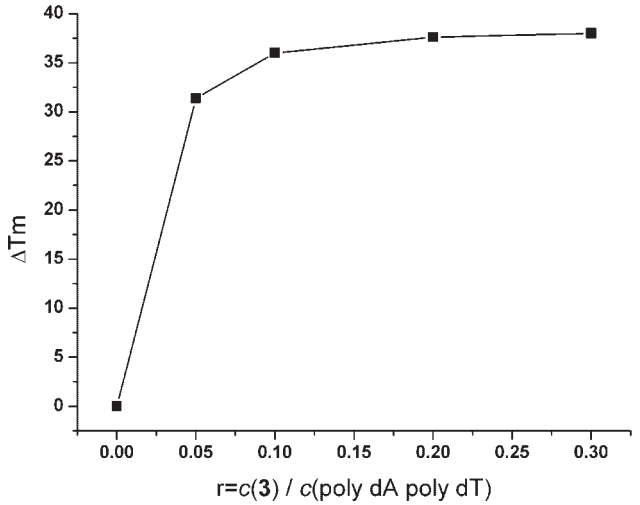

Figure 5. Non-linear dependence of ratio *r* (molar ratio of **3**/nucleic acid phosphates) and respective ΔT_m values found for poly dA-poly dT at pH = 5 (sodium citrate buffer, $I = 0.03\ \text{mol dm}^{-3}$)

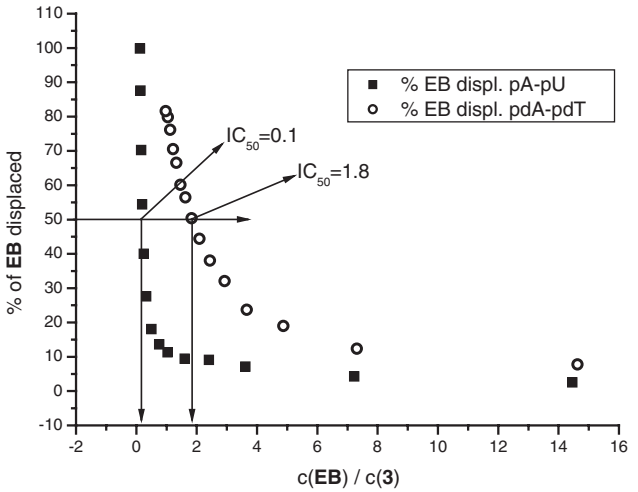

Figure 6. Ethidium bromide (**EB**) displacement assay: to ethidium bromide (c(**EB**) = $5 \times 10^{-6}\ \text{mol dm}^{-3}$) solution polynucleotide ($c = 6 \times 10^{-5}\ \text{mol dm}^{-3}$, r[**EB**]/[polynucleotide] = 0.08) was added, and quenching of the **EB**/polynucleotide fluorescence emission ($\lambda_{ex} = 500$ nm, $\lambda_{em} = 595$ nm (RNA) and $\lambda_{em} = 605$ nm (DNA)) was monitored as function of increasing c(**EB**)/c(**3**)

For all ds-polynucleotides, increase of the ratio r did not result in a proportional increase of ΔT_m values (Fig. 5). According to this non-linearity (dependence of ΔT_m values on the ratio r; Table 3), saturation of binding sites could be estimated at about $r \approx 0.2$,[20] the value being in accordance with calculated values for the ratio $n_{[\text{bound 3}]/[\text{polynucleotide}]}$ from the spectrophotometric titrations (Table 2). This finding does not support bis-intercalative binding mode.

Ethidium bromide (EB) displacement assays. The results of fluorimetric titrations (Table 2) and thermal denaturation experiments (Table 3) pointed towards opposite stabilities of complexes, former method suggesting higher stability of **3**/polyA-poly U complex than **3**/polydA-poly dT complex and latter method resulting in the significantly lower stabilisation of polyA-poly U if compared to the DNA analogue. Therefore, we have performed **EB** displacement assay as an alternative method for the estimation of affinity, since it is based on the ability of studied molecule to compete for the intercalation binding site with classical intercalator (Fig. 6).[21]

It should be taken into account that applied ratios $r_{[3]/[\text{polynucleotide}]}$ and concentration range of **3** and polynucleotides are comparable with thermal denaturation experiments. The IC_{50} value of **3** (Figure 6) showed that **3** efficiently displaced **EB** from poly dA-poly dT, pointing to the comparable affinity of **EB** and **3** towards DNA polynucleotide. This result is in accordance with the value of binding constant (K_s) obtained for **3** and previously reported for **EB**[10] and it is also supported by strong stabilisation of double helix of poly dA-poly dT by **3** (Table 3). More than one order of magnitude lower IC_{50} value of **3** obtained for **EB** displacement from polyA-poly U (Fig. 6) is in agreement with significantly lower stabilisation effect (positive ΔT_m value, Table 3) if compared to poly dA-poly dT stabilisation (Table 3).

CD spectroscopy. So far, non-covalent interactions at 25°C were studied by monitoring the spectroscopic properties of studied compound upon addition of the polynucleotides. In order to get insight into the changes of polynucleotide properties induced by small molecule binding, we have chosen CD spectroscopy as a highly sensitive method towards conformational changes in the secondary structure of polynucleotides.[22] In addition, achiral small molecules can eventually acquire induced CD (ICD) spectrum upon binding to polynucleotides, which could give useful information about modes of interaction.[22] The representative CD titration experiments are shown at Figs. 7–9.

In the CD spectra of ct-DNA and poly dA-poly dT (Figures 7, 8), pronounced decrease of peaks at 275 nm and 283 nm, respectively, was found to be proportional to the increasing concentration of **3**, strongly supporting **3**/polynucleotide complex formation.[22] In addition, new, strongly negative band appeared at 235 nm, which can be attributed to the ICD spectrum[22] of **3** (see UV/vis data, Chapter 2.2). Other ICD bands, which could be expected at $\lambda > 350$ nm, are not visible due to the low ε values. Interestingly, band at 235 nm is more pronounced at lower ratios $r = 0.2$–0.4 than at ratios close to equimolar concentrations of **3** and polynucleotide (Figs 7b and 8b). This observation is in good accordance with the calculated values of Scatchard ratio n (Table 2), as well as with proposed intercalative binding mode. Namely, at condition of excess of DNA intercalation binding sites over concentration of **3** ($r = 0$–0.25), most of the studied

DOI: 10.1002/poc

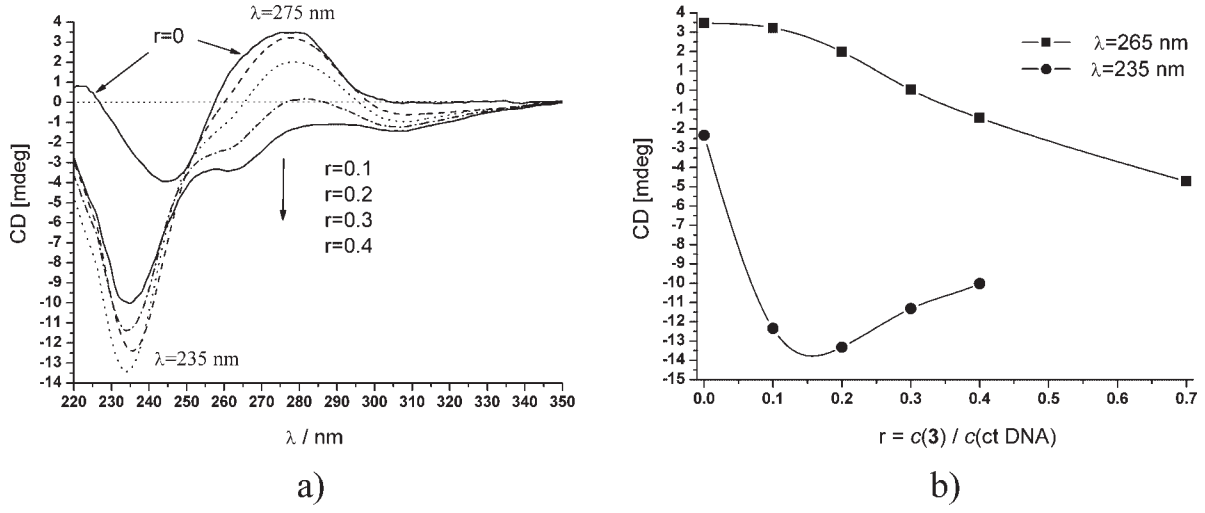

Figure 7. CD titration of ct-DNA ($c = 4.6 \times 10^{-5}$ mol dm^{-3}) with **3** at pH 5 (sodium citrate buffer, $I = 0.03$ mol dm^{-3}); (a) changes in complete spectra; (b) dependence of changes at specific bands on a molar ratio $r = [\mathbf{3}]/[\text{ct-DNA}]$

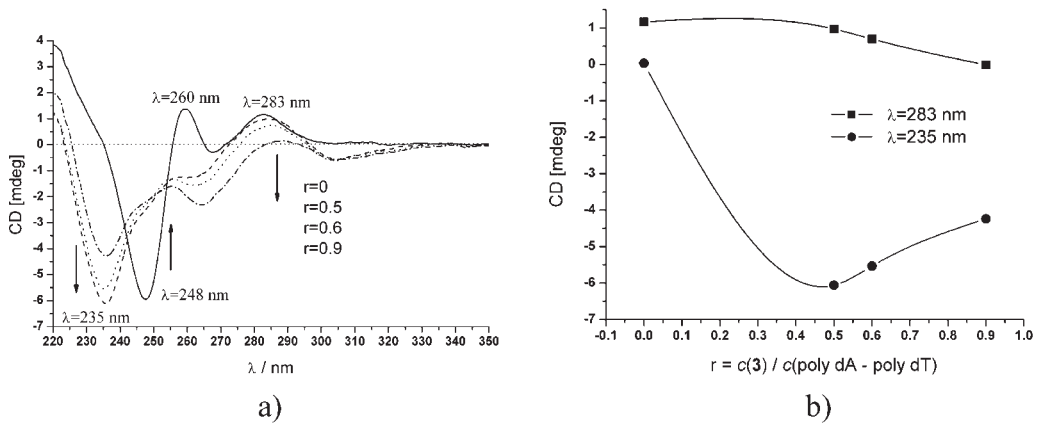

Figure 8. CD titration of poly dA-poly dT ($c = 2.7 \times 10^{-5}$ mol dm^{-3}) with **3** at pH 5 (sodium citrate buffer, $I = 0.03$ mol dm^{-3}); (a) changes in complete spectra; (b) dependence of changes at specific bands on a molar ratio $r = [\mathbf{3}]/[\text{poly dA-poly dT}]$

molecules bind by intercalation, consequently are similarly oriented and acquire ICD spectrum characterised by strongly negative band at 235 nm. At condition of excess of **3** over intercalation binding sites ($r = 0.3$–1), the equilibrium is probably shifted in favour of hydrophobic molecules of **3** aggregating within the grooves of DNA double helix, thus resulting in less pronounced ICD band at 235 nm.

Titration of poly A-poly U with **3** yielded also strong decrease of peak at 265 nm, similar to corresponding changes observed for DNA polynucleotides (peaks at 275 and 283 nm). However, the ICD band at 235 nm (present in titrations of DNA polynucleotides with **3**, Figs. 7 and 8) is not observed in the titration of poly A-poly U with **3** (Fig. 9). Absence of the measurable ICD band suggested that most of the molecules of **3** are not uniformly oriented in regard to RNA double stranded helix. This is in accordance with results of thermal melting experiments and fluorimetric titrations, which point towards more co-existing binding modes. Such disruption of RNA chirality could correspond to the RNA destabilisation observed in the thermal denaturation experiments (Table 3).

Discussion of the results of interactions between 3 and polynucleotides

According to the changes in fluorescence spectrum of **3** induced by addition of polynucleotides, significantly lower concentration of polyA-poly U led to the saturation when compared to the concentration of the poly dA-poly dT and other DNA polynucleotides necessary for accomplishing comparable changes. Such observation suggested higher stability of **3**/poly A-poly U complex or more complexes formed simultaneously. Thermal denaturation experiments pointed to co-existence of two different **3**/poly A-poly U complexes at studied ratio *r*, one being thermally less stable and the other more stable than free poly A-poly U. Complex characterised by

DOI: 10.1002/poc

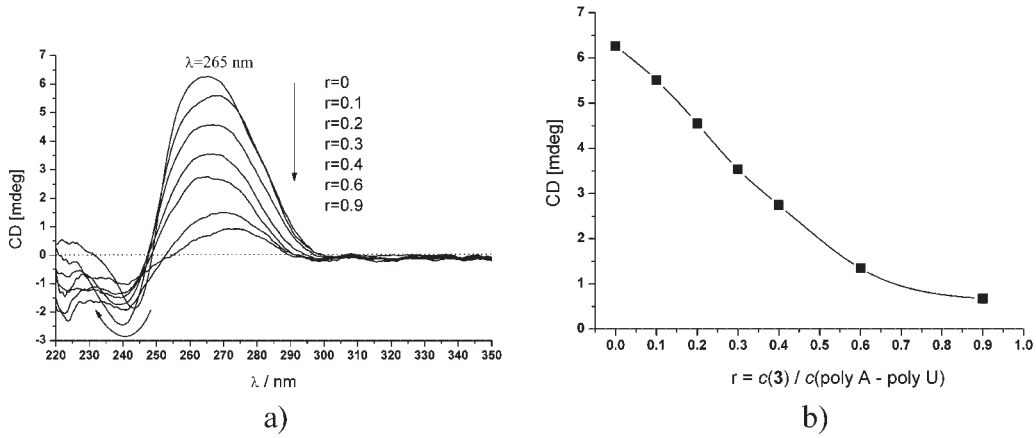

Figure 9. CD titration of poly A-poly U ($c = 4.0 \times 10^{-5}$ mol dm^{-3}) with **3** at pH 5 (sodium citrate buffer, $I = 0.03$ mol dm^{-3}); (a) changes in complete spectra; (b) dependence of changes at specific band on a molar ratio $r = [\mathbf{3}]/[\text{poly A-poly U}]$

positive ΔT_m value could be attributed to the intercalative binding mode but destabilisation (negative ΔT_m value) for sure cannot be the result of intercalation; thus, it is likely caused by some other binding event. At this point, we should take in account that fluorescence changes of **3** induced by polynucleotide addition are actually the sum of all interactions of the starting free **3** in the studied system. Possible interactions upon addition of polynucleotide consist not only of **3**/polynucleotide interactions but also intermolecular interactions between two or more molecules of **3** in the hydrophobic micro-environment of one of the polynucleotide grooves are possible to occur. Such aggregation of **3** in one of the poly A-poly U grooves would also explain the absence of ICD band in the CD titration experiments since the aggregates of chromophores of **3** cannot be uniformly oriented in regard to polynucleotide double helix. Pronounced ICD band of **3** observed exclusively in the experiments with DNA polynucleotides additionally supported intercalative binding mode, while disruption of chirality of RNA upon addition of **3** without any measurable ICD band pointed towards dominant non-intercalative binding of **3** at conditions close to the equimolar **3**/RNA phosphates ratio. Such disruption of RNA chirality could correspond to the RNA destabilisation observed in the thermal denaturation experiments.

Since it is well known that ds-DNA and ds-RNA by most differ in β-helical structure of former characterised by deep, narrow minor groove and broad, shallow major groove and α-helical structure of latter having roughly opposite properties of corresponding grooves,[2] the pronounced DNA over RNA selectivity of **3** pointed towards significant impact of polynucleotide secondary structure on the non-covalent interactions with **3**. Based on these structural differences, we propose for **3**/poly dA-poly dT and other **3**/DNA complexes mono-intercalative binding mode from the minor groove position, additionally stabilised by electrostatic and hydrophobic interactions of the non-intercalated part of the **3** in deep, narrow minor groove. On the other hand, **3** formed at least two different complexes with poly A-poly U. For one of them, we propose mono-intercalative binding of **3** with less efficient additional interactions of non-intercalated part of **3** in the broad and shallow minor groove, resulting in low but still positive thermal stabilisation of poly A-poly U and low IC_{50} values. For other type of complex, we propose aggregation of **3** in one of the grooves of poly A-poly U, yielding strong effect on the fluorescence spectra of the free **3** but having small (thermally destabilising) effect on the poly A-poly U. Such low affinity complex could be formed only at excess of **3** over poly A-poly U intercalation binding sites, what is actually observable from thermal stabilisation experiments—positive (intercalation) ΔT_m value is stable over the studied range of ratio *r*, while increased destabilising effect (aggregation of **3** in major groove) is proportional to the increased ratio *r*. In accord with that low IC_{50} value is observed for such $\mathbf{3}_{aggregated}$/polyA-poly U complex, since $\mathbf{3}_{aggregated}$ obviously does not compete significantly with the binding of **EB** to intercalation binding sites of poly A-poly U.

PHARMACOLOGY

Cell growth inhibition

Since all bis-4,9-diazapyrenium analogues prepared till now **3**, **5** and **6** have shown strong affinity towards DNA and RNA, and their monomers demonstrated considerable antiproliferative effects on human cell lines,[8] it was interesting to explore antiproliferative potential of **3**, **5** and **6** against a panel of cultured human tumour cell lines. As presented on Fig. 10, tested compounds showed weak (0–20%) to high potency (50–70%) of cytotoxicites on tumour cell lines, depending on applied dose of tested compound and treated cell line.

DOI: 10.1002/poc

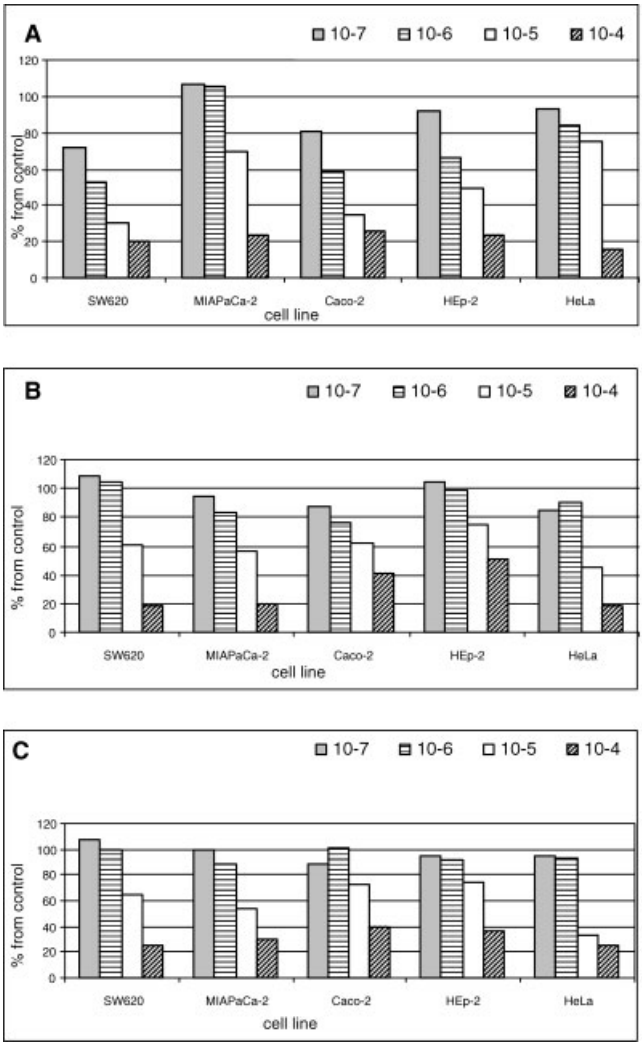

Figure 10. The growth inhibitory effect of bis-4,9-diazapyrenium analogues **3** (A), **5** (B) and **6** (C) on human tumour cells. The treated tumour cell growth inhibition was calculated relative to growth of untreated (control) cells and shown as per cent (%). Human cell lines: cervical adenocarcinoma (HeLa), larynx carcinoma (HEp2), colon carcinoma (Caco2), poorly differentiated cells from lymph node metastasis of colon carcinoma (SW-620), and pancreatic adenocarcinoma (MIAPaCa2). Exponentially growing cells were treated with different concentration (10^{-7} M to 10^{-4} M) of analogues during 72-h period. Cytotoxicity was analysed with MTT survival assay

In the applied concentration of 10^{-7} mol dm^{-3} to 10^{-4} mol dm^{-3}, analogue **3** demonstrated stronger growth inhibition effects against HEp2, SW-620 and Caco-2 cells (Fig. 2A) in comparison to analogues **5** and **6** (Fig. 2B,C). At the same condition cervical carcinoma cells-HeLa were more sensitive to analogues **5** and **6** compared to **3**. All three tested compounds displayed same growth inhibitory potential against MIAPaCa2 cells (Fig. 10). In general, differences in activity of **3**, **5**, and **6** towards different cell lines are not significant enough to point towards different modes of action. Moreover, growth inhibitory effect of bis-4,9-diazapyrenium is quite comparable to effect obtained for their monomers.[8] This observation, together with the afore described DNA/RNA binding assays, strongly suggests that studied compounds owe their antiproliferative activity to the interactions with DNA and/or RNA within the cell.

CONCLUSIONS

Novel bis-4,9-diazapyrenium dications **3** and **4**, same as previously studied bis-4,9-diazapyrenium analogues **5** and **6**, form complexes with the nucleotides of 1:1 and 1:2 stoichiometry, exhibiting no chelate effect, thus each 4,9-diazapyrenium unit binding one molecule of nucleotide independently. Stability constant values (K_s) of **4**/nucleotide complexes are dependent on the size of the aromatic surface of nucleobase pointing towards π–π aromatic stacking interactions between **4** and nucleotides as dominant binding interactions. Although structural properties of **3** and **4** allow easy insertion of two base pairs between diazapyrenium units, **3** and **4** bind to double stranded DNA most likely by mono-intercalative mode with additional interactions of non-intercalated unit. Observed strong DNA over RNA selectivity in ΔT_m values of **3** is common for most of the intercalators. The ICD band of **3** was observed exclusively for ds-DNA polynucleotides and not for RNA analogues, thus offering application of **3** as ds-DNA specific probe. In general, bis-4,9-diazapyrenium dications **3**, **5**, and **6** exhibited strong antiproliferative potential against human tumour cell lines but comparable to their monomeric analogues,[8] suggesting similar mechanism of action by interactions with cell DNA. In addition, bis-4,9-diazapyrenium di-cations exhibit reversible ring opening (see chapter 2.3) at weakly acidic conditions (pKa ≈ 6) and thus hold some promise as compounds targeting different acidic solid tumour tissues,[23] since pH reversible change of previously studied 4,9-diazapyrenium monomers was marked as the possible cause of the observed selectivity towards tumour cell lines.[8] The fluorescence of the 4,9-diazapyrenium system is strongly dependent on the reversible ring opening, thus allowing usage of 4,9-diazapyrenium cations' pH sensitive fluorescent probes.

EXPERIMENTAL

Synthesis of 2,2′-(methylenedibenzyl) -bis-(4,9-diazapyrenium) dibromide (3)

Solution of 4,9-diazapyrene **1** (0.15 g, 0.735 mmol) and bis[4-(bromomethyl)phenyl]methane **2** (0.118 g, 0.334 mmol) in dry acetonitrile was refluxed in the dark at 60–70°C for 22 h. The light-brown precipitate formed was washed with dry acetonitrile and dried under reduced pressure in the dark to give **3** in 84% yield. Figure 11

DOI: 10.1002/poc

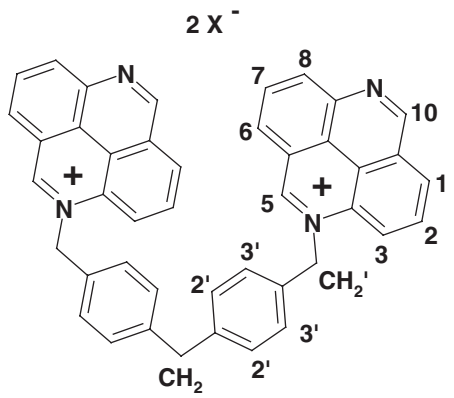

Figure 11. Proton annotation of the 2,2′-(methylenedibenzyl)-bis-(4,9-diazapyrenium) dication

^{1}H NMR(DMSO-d_6): 3.89(s, 2H—CH_2); 6.52(s, 4H—CH_2'); 7.23(d, $J_{2'3'} = 8.0$ Hz, 4H—C2′); 7.52(d, $J_{3'2'} = 8.0$ Hz, 4H—C3′); 8.59(dd, $J_{23} = J_{21} = 8$ Hz 2H—C2); 8.59(dd, $J_{23} = J_{21} = 8$ Hz 2H—C2); 8.98(d, $J_{12} = 8$ Hz 2H—C1); 9.05(d, $J_{31} = 8$ Hz 2H—C3); 9.12–9.17(2dd, 4H—C6, C8); 10.04(s, 2H—C10); 11.02(s, 2H—C5). ESI-MS: calculated (found): $C_{43}H_{32}N_{42}^+$ Br^- (—Br^-) 681.1454 (681.0202); $C_{43}H_{32}N_{42}^+$(—2Br^-) 602.2471 (602.1449).

Conversion to dichloride (4)

Dibromide **3** (0.15 g, 0.2 mmol) and freshly prepared AgCl (0.5 g, 3.5 mmol) were suspended in water and heated at 100°C in the dark for 2 h under vigorous stirring. After cooling, the formed AgBr and excess of AgCl were separated using a centrifuge. Aqueous solution was evaporated to dryness and dark-brown residue re-crystallised from a small volume of hot methanol giving light-brown precipitate of **4** at 76% yield.

^{1}H NMR(D_2O): 3.8(s, 2H—CH_2); 5.78(s, 4H—CH_2'); 7.3(d, $J_{2'3'} = 7.95$ Hz, 4H—C2′); 7.41(d, $J_{3'2'} = 7.95$ Hz, 4H—C3′); 7.52–7.68 (m, 6H—C1, C7, C8); 7.78(dd, $J_{23} = 8.3$Hz, $J_{21} = 8$ Hz 2H—C2); 7.95–8(d and s, 4H—C6 and C10); 8.41(d, $J_{32} = 8.3$Hz, 2H—C3); 9.79(s, 2H—C5). ESI-MS: calculated (found): $C_{43}H_{32}N_4^{2+}$ Cl^- (—Cl^-) 637.2159 (637.3672); $C_{43}H_{32}N_4^{2+}$(—2Cl^-)602.2471 (602.1526); $C_{29}H_{24}N_2^+$ (—DAP—CH_2, —2Cl^-) 398.1783 (398.1753).

Materials and methods

^{1}H-NMR spectra were recorded on Bruker spectrometers at 300 and 600 MHz. Chemical shifts (δ) in ^{1}H NMR spectra are expressed in ppm and J values in Hz. The NMR measurements were done in DMSO-d_6 using TMS as an internal standard or in D_2O solution using water signal as reference. Signal multiplicities are denoted as s (singlet), d (doublet), t (triplet), q (quartet) and m (multiplet). Electronic absorption spectra were obtained on Varian Cary 100 Bio spectrometer and fluorescence spectra were recorded on a Varian Cary Eclipse and Perkin Elmer LS 50 fluorimeter, while CD spectra were collected on JASCO J815 spectrometer; for all methods quartz cuvettes (1 cm) were used. The ESI-MS spectra were obtained using Waters Micromass ZQ. All measurements were performed in aqueous buffered solutions at pH = 5 (sodium citrate buffer, $I = 0.03$ mol dm^{-3}). Polynucleotides were purchased as noted: poly A-poly U, poly dA-poly dT, poly dAdT-poly dAdT, poly dGdC-poly dGdC (Sigma), calf thymus ct-DNA (Aldrich). Polynucleotides were dissolved in sodium cacodylate buffer, $I = 0.05$ mol dm^{-3}, pH = 7. Calf thymus ct-DNA was additionally sonicated and ltered through a 0.45 μm lter.[9] Polynucleotide concentration was determined spectroscopically, and expressed as concentration of backbone phosphates. Fluorimetric and UV/vis titrations were performed by adding portions of polynucleotide solution into the solution of the studied compound, while CD experiments were by adding aliquots of studied compound to the polynucleotide solution. Absorbance and fluorescence emission of **3** and **4** were proportional to their concentration under the experimental conditions. Titration data were corrected for dilution. Excitation of **3**, **4** at $\lambda_{max} = 332$ nm was used for fluorimetric titrations since nucleotides and polynucleotides do not absorb light at $\lambda > 300$ nm and fluorescence spectra partially overlap with electronic absorption maxima at $\lambda_{max} > 360$ nm. Binding constants (K_s) for **4**/nucleotide complexes were calculated by SPECFIT program from fluorimetric titration data.[13] Processing of titration data by means of Scatchard equation[16,17] was used for calculation of ratio n (bound **3**,**4**]/[polynucleotide]) and binding constants (K_s) for **3**,**4**/polynucleotide complexes. Obtained values for K_s and n all have satisfactory correlation coefficients (>0.999). Thermal melting curves for DNA, RNA, and their complexes with **3** were determined as previously described by following the absorption change at 260 nm as a function of temperature.[24] Absorbance of **3** was subtracted from every curve, and the absorbance scale was normalised. T_m values are midpoints of the transition curves, determined as maximum of the first derivative plots and checked graphically by the tangent method. ΔT_m values were calculated subtracting T_m of the free nucleic acid from T_m of the complex. Every ΔT_m value here reported was the average of at least two measurements; the error in ΔT_m is ± 0.5°C.

Antitumour activity assays

Materials for biological testing. The Dulbecco's modified Eagle medium (DMEM) with 10% foetal bovine serum (FBS) and trypsin-EDTA were purchased from Institute of Immunology Inc. (Zagreb, Croatia); 3-(4,5-dimethyl-2-thiazolyl-2H-tetrazolium bro-

DOI: 10.1002/poc

mide (MTT) and dimethylsulfoxyde (DMSO) were purchased from Merck (Darmstadt, Germany). Glutamine, penicillin, streptomycin, and all others chemicals were obtained from Sigma Chem. Co. (St. Louis, USA).

Cytotoxicity against human tumour cells. The cytotoxic activities of bis-4,9-diazapyrenium analogues **3**, **5**, and **6** were investigated on human tumour cell lines. Human cervical adenocarcinoma cells (HeLa), human larynx carcinoma cells (HEp2), human colon carcinoma cells (Caco2), poorly differentiated cells from lymph node metastasis of colon carcinoma (SW-620), and human pancreatic adenocarcinoma cells (MIAPaCa2) were grown as a monolayer in tissue culture flasks (250 ml; BD Falcon, Germany) in DMEM with 10% FBS supplemented with 2 mM glutamine, 100 U of penicillin and 0.1 mg streptomycin. Cells were cultured in a humidified (95% air, 5% CO_2) CO_2 incubator (Shell Lab, Sheldon Manufacturing, USA) at 37°C. The trypan blue dye exclusion method was used to assess cell viability. Cytotoxic effects on the tumour cell growth were determined using the MTT assay.[25] In general, compounds were dissolved in warm water and all working dilutions (10^{-3}–10^{-6} M) were prepared immediately before each experiment. Tumour cells, 2×10^4 cells/ml, were plated onto 96-microwell plates (Costar, Cambridge, USA) and allowed to attach overnight in a CO_2 incubator (Shell Lab, Sheldon Manufacturing, USA). Twenty-four hours later, different concentrations of investigated compounds into each well were added. Controls were grown under the same conditions without the addition of the test substances. After 72 h of incubation, medium was removed and 40 μl of MTT (5 mg/ml of phosphate buffered saline) was added. After 4 h of incubation, MTT-formazane crystals were dissolved in DMSO. The plates were transferred to an Elisa plate reader (Stat fax 2100, Pharmacia Biotech, Uppsala Sweden). Absorbance was measured at 570 nm. All experiments were performed at least three times, with three wells each.

Acknowledgements

Support for this study by the Ministry of Science, Education and Sport of Croatia is gratefully acknowledged (Projects 0098053, 0127111).

REFERENCES

1. (a) Hertzberg RP. In *Comprehensive Medicinal Chemistry*, vol. 2, Hansch C, Sammes PG, Taylor JB (eds). Pergamon: Oxford, 1990; pp 753–791;; (b) Ralph RK, Judd W, Kohn KW. In *Molecular Aspects of Anticancer Drug—DNA Interactions*, vol. 2, Neidle S, Waring M (eds). CRC: Boca Raton FL, 1994;; (c) Wilson WD. In *Nucleic Acids in Chemistry and Biology*. 2nd edition, Blackburn M, Gait M (eds). IRL Press: Oxford, 1996.
2. (a) Demeunynck M, Bailly C, Wilson WD. In *DNA and RNA Binders*. Wiley-VCH: Weinheim, 2002;; (b) Saenger W. In *Principles of Nucleic Acid Structure*. Springer: New York, 1988.
3. (a) Luedtke NW, Liu Q, Tor Y. *Bioorg. Med. Chem.* 2003; **11**: 5235–5247;; (b) Luedtke NW, Hwang JS, Nava E, Gut D, Kol M, Tor Y. *Nucleic Acids Res.* 2003; **31**: 5732–5740.
4. Kubar T, Hanus M, Ryjacek F, Hobza P. *Chem. Eur. J.* 2005; **12**: 280–290.
5. (a) Luedtke NW, Liu Q, Tor Y. *Chem. Eur. J.* 2005; **11**: 495–508;; (b) Tam VK, Liu Q, Tor Y. *Chem. Commun.* 2006; 2684–2686.
6. (a) Blacker J, Jazwinski J, Lehn J-M. *Helv. Chim. Acta* 1987; **70**: 1–11;; (b) Blacker J, Jazwinski J, Lehn J-M, Wilhelm FX. *J. Chem. Soc., Chem. Commun.* 1986; 1035;; (c) Slama-Schwok A, Jazwinski J, Bere A, Montenay-Garestier T, Rougge M, Hélène C, Lehn J-M. *Biochemistry* 1989; **8**: 3227–3234;; (d) Slama-Schwok A, Rougge M, Ibanez V, Geacintov NE, Montenay-Garestier T, Lehn J-M, Hélène C. *Biochemistry* 1989; **8**: 3234–3242;; (e) Brun AM, Harriman A. *J. Am. Chem. Soc.* 1991; **113**: 8153–8159;; (f) Coudret C, Harriman A. *J. Chem. Soc. Chem. Commun.* 1992; 1755–1757.
7. Piantanida I, Tomišić V, Žinić M. *J. Chem. Soc., Perkin Trans. 2* 2000; 375–383.
8. (a) Yu D-H, MacDonald J, Josephs S, Liu Q, Nguy V, Tor Y, Wong-Staal F, Li Q-X. *Invest. New Drugs* 2006; **24**: 489–498;; (b) Steiner-Biočić I, Glavaš-Obrovac Lj, Karner I, Piantanida I, Žinić M, Pavelić K, Pavelić J. *Anticancer Res.* 1996; **16**: 3705–3708;; (c) Roknić S, Glavaš-Obrovac Lj, Karner I, Piantanida I, Žinić M, Pavelić K. *Chemotherapy* 2000; **46**: 143–148;; (d) Marczi S, Glavaš-Obrovac Lj, Karner I. *Chemotherapy* 2005; **51**: 217–222.
9. Palm BS, Piantanida I, Žinić M, Schneider H-J. *J. Chem. Soc., Perkin Trans. 2* 2000; 385–392.
10. Piantanida I, Palm BS, Žinić M, Schneider H-J. *J. Chem. Soc., Perkin Trans. 2* 2001; 1808–1816.
11. (a) Kuruvilla E, Joseph J, Ramaiah D. *J. Phys. Chem. B* 2005; **109**: 21997–22002;; (b) Joseph J, Eldho NV, Ramaiah D. *Chem. Eur. J.* 2003; **9**: 5926–5935;; (c) Carrasco C, Helissey P, Haroun M, Baldeyrou B, Lansiaux A, Colson P, Houssier C, Giorgi-Renault S, Bailly C. *Chem. Bio. Chem.* 2003; **4**: 50–61;; (d) Bolognesi ML, Andrisano V, Bartolini M, Banzi R, Melchiorre C. *J. Med. Chem.* 2005; **48**: 24–27.
12. Mosby WL. *J. Org. Chem.* 1957; **22**: 671–673.
13. Specfit Global Analysis, a program for fitting, equilibrium and kinetic systems, using factor analysis & Marquardt minimization; (a) Gampp H, Maeder M, Meyer CJ, Zuberbuehler AD. *Talanta* 1985; **32**: 257–264;; (b) Maeder M, Zuberbuehler AD. *Anal. Chem.* 1990; **62**: 2220–2224.
14. Dougherty G, Pilbrow JR. *Int. J. Biochem.* 1984; **16**: 1179–1192.
15. Pal MK, Ghosh JK. *Spectrochim. Acta Part A* 1995; **51**: 489–498.
16. Scatchard G. *Ann. N. Y. Acad. Sci.* 1949; **51**: 660–672.
17. McGhee JD, von Hippel PH. *J. Mol. Biol.* 1976; **103**: 679–684.
18. Wakelin JPG. *Med. Res. Rev.* 1986; **6**: 275–340.
19. Cantor CR, Schimmel PR. In *Biophysical Chemistry*, vol. 3. Freeman WH, and Co.: San Francisco, 1980;
20. Wilson WD, Tanious FA, Fernandez-Saiz M, Rigl CT. In *Evaluation of Drug/Nucleic Acid Interactions by Thermal Melting Curves: Methods in Molecular Biology*, vol. 90, *Drug-DNA Interaction Protocols*, Fox KR (ed.). Humana Press Inc.: Totowa, NY, 1998.
21. Boger DL, Fink BE, Brunette SR, Tse WC, Hedrick MP. *J. Am. Chem. Soc.* 2001; **123**: 5878–5891.
22. Rodger A, Norden B. In *Circular Dichroism and Linear Dichroism*. Oxford University Press: New York, 1997;
23. Raghunand N, Gillies RJ. *Drug Resist. Updat.* 2000; **3**: 39–47.
24. Chaires JB, Dattagupta N, Crothers DM. *Biochemistry* 1982; **21**: 3933–3940.
25. Horiuchi N, Nakagawa K, Sasaki Y, Minato K, Fujiwara Y, Nezu K, Ohe Y, Saijo N. *Cancer Chemother. Pharmacol.* 1988; **22**: 246–250.

DOI: 10.1002/poc